

# Characterization of biological pathways associated with a 1.37 Mbp genomic region protective of hypertension in Dahl S rats

Allen W. Cowley, Jr., Carol Moreno, Howard J. Jacob, Christine B. Peterson, Francesco C. Stingo, Kwang Woo Ahn, Pengyuan Liu, Marina Vannucci, Purushottam W. Laud, Prajwal Reddy, Jozef Lazar, Louise Evans, Chun Yang, Theresa Kurth and Mingyu Liang

*Physiol. Genomics* 46:398-410, 2014. First published 8 April 2014;  
doi:10.1152/physiolgenomics.00179.2013

---

## You might find this additional info useful...

---

Supplemental material for this article can be found at:

</content/suppl/2014/04/16/physiolgenomics.00179.2013.DC1.html>

This article cites 78 articles, 29 of which can be accessed free at:

</content/46/11/398.full.html#ref-list-1>

Updated information and services including high resolution figures, can be found at:

</content/46/11/398.full.html>

Additional material and information about *Physiological Genomics* can be found at:

<http://www.the-aps.org/publications/pg>

---

This information is current as of June 16, 2014.

## Characterization of biological pathways associated with a 1.37 Mbp genomic region protective of hypertension in Dahl S rats

Allen W. Cowley, Jr.,<sup>1</sup> Carol Moreno,<sup>1,2</sup> Howard J. Jacob,<sup>1,2</sup> Christine B. Peterson,<sup>6</sup> Francesco C. Stingo,<sup>5</sup> Kwang Woo Ahn,<sup>3</sup> Pengyuan Liu,<sup>4</sup> Marina Vannucci,<sup>6</sup> Purushottam W. Laud,<sup>3</sup> Prajwal Reddy,<sup>2</sup> Jozef Lazar,<sup>2</sup> Louise Evans,<sup>1</sup> Chun Yang,<sup>1</sup> Theresa Kurth,<sup>1</sup> and Mingyu Liang<sup>1</sup>

<sup>1</sup>Department of Physiology, Medical College of Wisconsin, Milwaukee, Wisconsin; <sup>2</sup>Human and Molecular Genetics Center, Medical College of Wisconsin, Milwaukee, Wisconsin; <sup>3</sup>Division of Biostatistics, Medical College of Wisconsin, Milwaukee, Wisconsin; <sup>4</sup>Cancer Center, Medical College of Wisconsin, Milwaukee, Wisconsin; <sup>5</sup>Department of Biostatistics, MD Anderson Cancer Center, Houston, Texas; and <sup>6</sup>Department of Statistics, Rice University, Houston, Texas

Submitted 4 December 2013; accepted in final form 2 April 2014

**Cowley AW Jr, Moreno C, Jacob HJ, Peterson CB, Stingo FC, Ahn KW, Liu P, Vannucci M, Laud PW, Reddy P, Lazar J, Evans L, Yang C, Kurth T, Liang M.** Characterization of biological pathways associated with a 1.37 Mbp genomic region protective of hypertension in Dahl S rats. *Physiol Genomics* 46: 398–410, 2014. First published April 8, 2014; doi:10.1152/physiolgenomics.00179.2013.—The goal of the present study was to narrow a region of chromosome 13 to only several genes and then apply unbiased statistical approaches to identify molecular networks and biological pathways relevant to blood-pressure salt sensitivity in Dahl salt-sensitive (SS) rats. The analysis of 13 overlapping subcongenic strains identified a 1.37 Mbp region on chromosome 13 that influenced the mean arterial blood pressure by at least 25 mmHg in SS rats fed a high-salt diet. DNA sequencing and analysis filled genomic gaps and provided identification of five genes in this region, *Rfwd2*, *Fam5b*, *Astn1*, *Pappa2*, and *Tnr*. A cross-platform normalization of transcriptome data sets obtained from our previously published Affymetrix GeneChip dataset and newly acquired RNA-seq data from renal outer medullary tissue provided 90 observations for each gene. Two Bayesian methods were used to analyze the data: 1) a linear model analysis to assess 243 biological pathways for their likelihood to discriminate blood pressure levels across experimental groups and 2) a Bayesian graphical modeling of pathways to discover genes with potential relationships to the candidate genes in this region. As none of these five genes are known to be involved in hypertension, this unbiased approach has provided useful clues to be experimentally explored. Of these five genes, *Rfwd2*, the gene most strongly expressed in the renal outer medulla, was notably associated with pathways that can affect blood pressure via renal transcellular Na<sup>+</sup> and K<sup>+</sup> electrochemical gradients and tubular Na<sup>+</sup> transport, mitochondrial TCA cycle and cell energetics, and circadian rhythms.

Bayesian analysis; Dahl S rats; chromosome 13; pathway analysis; salt-sensitive hypertension

HYPERTENSION IN THE VAST MAJORITY of the human population is the consequence of one's genetic makeup and environmental factors. While genome-wide association studies have identified many candidate regions and genes, the genetic basis of the disease remains elusive. It is evident, however, that hypertension is polygenetic and single gene effects can account for only a small percent of the pressure phenotype (45). Among the environmental factors that can contribute to hypertension is dietary salt intake, which is directly correlated with the risk of

developing hypertension in both experimental animal models and in human populations (17, 37). Enhanced sensitivity of blood pressure to salt intake is present in nearly half of Americans who are afflicted with hypertension (61, 66, 76) and is especially high (75%) in African American hypertensive patients (4, 66). The underlying causes of salt sensitivity in essential hypertension remain elusive, although there is evidence that the difference between sodium-loaded and sodium-restricted blood pressures is a highly heritable trait (51, 68). However, there remains a lack of a clear mechanistic understanding at the molecular genetic level of salt-sensitive hypertension.

The Dahl salt-sensitive SS/JrHsdMcowi (SS) rat is an inbred rat strain selected for the sensitivity of blood pressure to dietary salt intake. It recapitulates in many ways the progression of human hypertension as exemplified in the African American population and has provided key insights of mechanisms and the genetic complexity underlying salt sensitivity (6, 23, 37, 44, 49). Studies in our laboratory have utilized the SS rat to carry out congenic mapping to identify blood pressure loci in the rat genome and found that chromosome 13 (chr 13) harbored four important nonoverlapping genomic regions that can significantly influence salt sensitivity in the SS rat (52). One of these four regions was a 13.11 Mbp segment of the Brown Norway (BN, resistant to hypertension) rat chr 13 (from position 73.37 to 86.48 Mbp) that when transferred into the SS background, attenuated salt-induced hypertension by at least 25 mmHg in male rats. Utilizing this congenic rat strain, we had two goals for the present study. First, to narrow this congenic region by developing multiple overlapping subcongenic strains for identification of causative genes and sequence variants within this congenic region. Second, to determine the relevance of the genes within the narrow region of interest in the context of molecular networks and pathways to translate genomic results into an integrated understanding of the complex pathways and mechanisms involved in the development of hypertension. The outer medulla was the focus of the present analysis since it is a major site of tubular and vascular dysfunction found to contribute to salt-sensitive hypertension in SS rats (9).

### METHODS

#### *Experimental Animals and Strain Nomenclature*

All studies utilized male SS rats and congenic strains derived from a cross between the consomic SS.13<sup>BN</sup> and SS rats. The congenic

Address for reprint requests and other correspondence: A. W. Cowley, Jr., Dept. of Physiology, Medical College of Wisconsin, 8701 Watertown Plank Rd., Milwaukee, WI 53226 (e-mail: acowley@mcw.edu).

strains were developed by marker-assisted breeding, as previously described (52). Rats from a previously described congenic strain SS.13<sup>BN26</sup> spanning a 13.1 Mbp congenic interval (from position 73.37–86.48 Mbp) (52) that was partially protected from the development of hypertension were back-crossed to SS rats to narrow the region and identify the causative genes and sequence variants. Rats in the F1 generation were intercrossed, and the progeny were genotyped with 20 microsatellite markers covering the entire 13.11 Mbp congenic interval (52, 53). Recombinant rats were selected as breeders for the establishment of 13 overlapping subcongenic strains. Flanking markers for each congenic strain are depicted in Fig. 1. All rats were bred and housed in an American Association for Accreditation of Laboratory Animal Care-accredited animal care facility at the Medical College of Wisconsin with free access to water and to a custom AIN-76A purified rodent chow (0.4% NaCl; Dyets, Bethlehem, PA). All experimental procedures were approved by the Institutional Care and Use Committee of the Medical College of Wisconsin.

*Phenotyping*

We surgically prepared 5–6 wk old male rats from the strains to be studied SS, SS.13<sup>BN</sup>, SS.13<sup>BN26</sup>, and 13 overlapping SS.13<sup>BN</sup> subcongenic (designated 26-A through 26-M) for the measurement of mean arterial pressure (MAP) and heart rate (HR) using radiotelemetry techniques as we have described (13, 19). Rats were anesthetized with 2.5% isoflurane and a gel-filled catheter implanted in the right carotid artery and the attached transmitter (DSI, Minneapolis, MN) secured subcutaneously between the scapulae. Postoperative administration of buprenorphine provided analgesia. After a 7-day recovery period, we then placed rats in metabolic cages without restricting food or water for an overnight urine collection to measure baseline proteinuria then returned to the home cage. Blood pressure was measured between 9 AM and 12 PM (“light cycle”) on three consecutive control days, and the dietary intake of NaCl increased from 0.4 to 8% for 14 days with hemodynamic measurements made on *days 1–3, 7, 10,* and

14 of high salt (HS) with a second overnight collection of urine following the measurements on the last day of HS. From urine collected, albumin was quantified using an Albumin Blue 580 (Molecular Probes) fluorescence assay. Proteinuria was quantified using Weichselbaum’s biuret reagent on an ACE auto-analyzer (Alfa Wassermann).

*Genomic DNA Sequencing of the 1.37 Mbp Candidate Region*

Ten bacterial artificial chromosome (BAC) genomic clones were obtained from BACPAC Resource Center of Children’s Hospital Oakland Research Institute, Oakland, CA (CHORI; <https://bacpac.chori.org>). These BACs, spanning the region, were generated from a single Brown Norway BN/NHsdMcwi (BN) by CHORI. DNA was extracted from 10 BAC clones spanning the 1.37 Mbp region by a modified Qiagen midiprep protocol. The sequencing of each BAC was performed with individual Single Molecule Real Time (SMRT) cells with a Pacific Biosciences (PacBio) RS sequencer (CA) following manufacturer’s protocol for circular consensus sequencing (CCS). The PacBio RS is capable of producing sequencing reads up to 5 kb in length. PacBio technology allows the sequencing of GC-rich and nucleotide repeat regions of the genome that Sanger or short read sequencing technology cannot sequence through. The ccs.fastq files created by the instrument’s base calling software were used for the secondary analysis pipeline. Secondary analysis was carried out using the RS\_Resequencing\_GATK protocol implemented in the PacBio SMRT Analysis package. Briefly, reads with raw read length > 50 bp and minimum accuracy of at least 75% were aligned to chr 13 reference of Rat assembly RGSC 5.0 (Rn5) using Basic Local Alignment with Successive Refinement (7). Base quality scores were recalibrated; consensus and variants were identified against the reference using Broad Institute’s GATK Unified Genotyper module. Sequence was analyzed as previously described (3).

The PacBio sequencing system yielded a mean depth of coverage of 200X, with a mean mapped read length of 1,760 bp. SS sequence

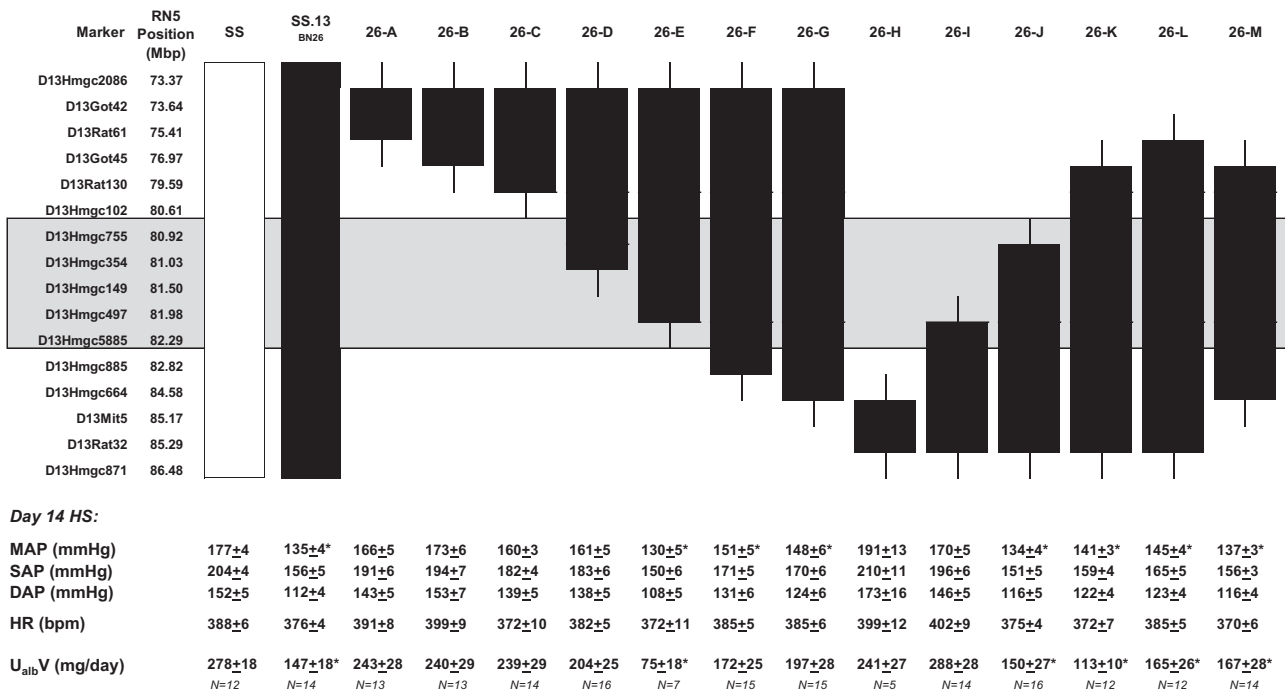


Fig. 1. Candidate region of chromosome 13 was reduced from 13.3 Mbp to 1.37 Mbp (position by RN5 genome assembly). The SS regions are indicated in white while the region derived from the Brown Norway (BN) is indicated in black. The narrowed region (1.37 Mbp) is shaded gray. Mean arterial pressure (MAP) on *day 14* of high salt (HS) for the 13 overlapping strains and the salt-sensitive (SS) and congenic SS.13<sup>BN26</sup> strains is given as well as the systolic arterial pressure (SAP), diastolic arterial pressure (DAP), heart rate [HR, in beats/min (bpm)], and albuminuria (U<sub>alb</sub>V) for the same day of HS. \*Significant differences from the SS strain on *day 14* HS for MAP *P* < 0.5.

was obtained with Illumina HiSeq, as described previously (27). Sequence comparison between BN and SS on the target region was performed with ANNOVAR (75).

#### RNA Expression

For the RNA-seq analysis, outer medullary tissue was collected and snap-frozen from the SS, congenic SS.13<sup>BN26</sup>, and five of the sub-congenic strains rats (26-D, 26-E, 26-I, 26-J, 26-M) rats at 7–8 wk of age. Each strain was maintained on an AIN-76A diet containing 0.4% salt or switched to 8% salt for 7 days prior to tissue collection. Tissues were collected after 7 days of HS to minimize the effects of the hypertension itself upon gene expression. Total RNA was extracted with Trizol reagent, and the quality of each sample assessed with Agilent 2100 BioAnalyzer to ensure an RNA Integrity Number > 0.8 (43). RNA samples of outer medullary tissue from three rats were pooled to yield three pooled samples for each strain and dietary condition for the current study as well as for the published studies included (42, 43). The pooled samples were used for RNA (cDNA) library preparation using Illumina's TruSeq RNA Sample Prep Kit (RS-122-2001) and sequenced using an Illumina HiSeq2000 sequencer as previously described (29). The 42 indexed libraries were multiplexed on two lanes of a flow-cell. RNA-seq analysis was performed on renal tissue with the goal of identifying pathways that might mediate the contributions of the genes residing in the 1.37 Mbp region to hypertension. Real-time polymerase chain reaction was used to quantify mRNA abundance of specific genes using SYBR Green chemistry (55).

#### Western Blot Analysis

Outer medullary tissue was homogenized, protein quantified, and lysates prepared as we have previously described (19, 69). Proteins were separated on a 10–20% Tris SDS-PAGE gel (Bio-Rad) and transferred to a PVDF membrane. Membranes were prepared and probed as we have described in detail (19). The antibody used for *Rfwd2* was Cop1 4466 (Genentech) used at a dilution of 1:200. A ChemiDoc imaging system (Bio-Rad) was used for documentation and analysis. The membrane was stained with Coomassie blue and then used to normalize the abundance of specific proteins as we have reported (71).

#### Normalization and Merging of Data Obtained From RNA-seq and Affymetrix GeneChip

Transcriptome studies are inevitably underpowered for traditional statistical analysis (77). To enhance the power of analysis, we obtained additional data points by merging the current RNA-seq dataset with our previously published RNA-seq and Affymetrix GeneChip data set (42, 43). The different rat strains, the diet, the number of RNA-seq libraries or GeneChips carried out in pooled samples ( $n = 3$  for each condition), and average levels of MAP ( $\pm$  SD) are summarized in Table 1. We studied 30 groups of rats of differing strains. Both the GeneChip and RNA-seq data were obtained from nine rats of each strain and per condition [low-salt (LS) and HS diet]. Three samples were pooled per rat strain at each salt diet condition. This provided 90 observations for each gene (e.g., three pooled samples per strain or condition  $\times$  30). Given the difference in scales of the data obtained from the two methods, a cross-platform normalization procedure [XPN method (64)] was used to construct a single unified dataset of 9,219 genes for which data were available from both platforms. Due to the skewedness of the original data, all measurements were first transformed by  $\log(1 + x)$ , where  $x$  is an original expression value. Specifically, Affymetrix GeneChip data are expressed as MAS-normalized log signal intensity values, and the RNA-seq data are expressed as fragments per kb of gene model per million total reads. The merged data not only achieved a common scale but also preserved the original data profile. Importantly, the

Table 1. Data included in the Bayesian analysis representing 90 RNA-seq libraries or GeneChips that were merged by a cross-platform normalization method that preserved the original data profile

Strain	Salt Diet	RNA-seq Libraries, <i>n</i> , or GeneChip	MAP, mmHg
<i>RNA-seq in current study</i>			
SS	8% 7 days	3	139 $\pm$ 9
SS	0.4%	3	107 $\pm$ 6
SS.13 <sup>BN26</sup>	8% 7 days	3	120 $\pm$ 8
SS.13 <sup>BN26</sup>	0.4%	3	101 $\pm$ 5
26-D	8% 7 days	3	133 $\pm$ 10
26-D	0.4%	3	109 $\pm$ 7
26-F	8% 7 days	3	123 $\pm$ 6
26-F	0.4%	3	106 $\pm$ 4
26-I	8% 7 days	3	131 $\pm$ 7
26-I	0.4%	3	104 $\pm$ 3
26-J	8% 7 days	3	116 $\pm$ 7
26-J	0.4%	3	102 $\pm$ 5
26-M	8% 7 days	3	120 $\pm$ 6
26-M	0.4%	3	103 $\pm$ 5
<i>Affymetrix GeneChip [Lu et al. (43)]</i>			
SS.13 <sup>BN</sup>	8% 3 days	3	107 $\pm$ 3
SS	8% 3 days	3	121 $\pm$ 7
SS.13 <sup>BN5</sup>	8% 3 days	3	119 $\pm$ 7
SS.13 <sup>BN26</sup>	8% 3 days	3	112 $\pm$ 6
SS.13 <sup>BN</sup>	8% 7 days	3	112 $\pm$ 4
SS	8% 7 days	3	131 $\pm$ 8
SS.13 <sup>BN5</sup>	8% 7 days	3	129 $\pm$ 10
SS.13 <sup>BN26</sup>	8% 7 days	3	118 $\pm$ 5
SS.13 <sup>BN</sup>	0.4%	3	99 $\pm$ 4
SS	0.4%	3	109 $\pm$ 5
SS.13 <sup>BN5</sup>	0.4%	3	107 $\pm$ 4
SS.13 <sup>BN26</sup>	0.4%	3	102 $\pm$ 3
<i>RNA-seq [Liu et al. (42)]</i>			
SS	4% 7 days	3	125 $\pm$ 11
SS	0.4%	3	107 $\pm$ 6
SS.13 <sup>BN26</sup>	4% 7 days	3	113 $\pm$ 7
SS.13 <sup>BN26</sup>	0.4%	3	104 $\pm$ 4

Mean arterial pressure (MAP)  $\pm$  SD.

merged data provided 90 biologically distinct data points for each gene for the Bayesian analyses.

#### Pathway Selection and Relationship of Candidate Genes to Genes Within Pathways Using Bayesian Analyses

Two recently developed analytical approaches were used to identify and prioritize biological pathways related to the candidate genes identified within the 1.37 Mbp candidate region of congenic SS.13<sup>BN26</sup>. First, pathways and genes related to blood-pressure salt sensitivity were identified by a Bayesian linear principal components analysis as we previously described (65, 77). The analysis incorporated information from all of the biological pathways from the KEGG database with three imposed constraints. First, the pathway needed to include its related member genes; second, the gene analyzed had to be included in a pathway that contained that gene; and third, selection of identical subsets of genes in different pathways was not allowed. A Markov chain Monte Carlo algorithm was implemented, which resulted in a set of pathways that were closely related to blood pressure. This resulted in a set of selected pathways and was followed by a graphical model analysis to infer relationships among the genes in those pathways. Specifically, a Bayesian approach was applied to estimate undirected graphical models, also known as Markov random fields, among sets of genes that overlapped with pathways of interest.

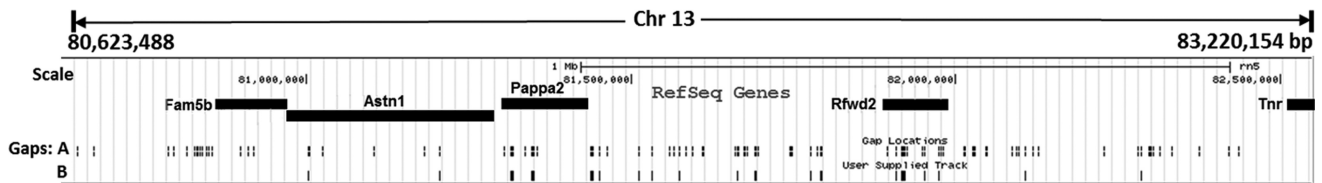


Fig. 2. Schematic of the genomic organization of the 1.37 Mbp region of the rat chromosome 13. Alignment of the PacBio reads against the reference genome was able to close the gaps from 78 (line A) to 19 gaps (line B) in the sequence. The 5 genes identified by RNA-seq are shown on this regional map (*Fam5b*, *Astn1*, *Pappa2*, *Rfwd2*, and *Tnr*).

Since the number of possible networks is exponential in the number of genes, it is not feasible to infer a network among all measured genes, both because of computational scaling issues and because of the limited sample size. Instead, the analysis focused on seven pathways selected by the procedure described above, as well as 10 KEGG pathways that had tractable size and were previously established as relevant to blood pressure regulation. Given computational limitations, the number of genes that were included in a large pathway (pathway #04080) was reduced to a manageable number based on the posterior probabilities of the genes obtained from the Bayesian linear principal components analysis described above. Another large pathway (pathway #04610) was divided into three biological subpathways. For each of these 19 pathways or subpathways, a graphical model inference was performed using the subset of genes from our data set, which overlapped with the given pathway, plus genes located in the 1.37 Mbp congenic region and showing detectable expression.

In an undirected graphical model, variables correspond to nodes and edges represent conditional dependence relationships, meaning that two variables are connected by an edge if and only if they are dependent after all other variables are accounted for. Since the data were distributed in a reasonably normal manner, a Gaussian graphical model (GGM) was used as has been previously used to infer gene association networks (15, 63). In a GGM, the conditional dependence relationships among gene expression levels correspond to constraints on the inverse covariance matrix of the multivariate normal distribution, known as the precision matrix. An entry in the precision matrix will be nonzero if and only if the corresponding variables are connected by an edge in the conditional dependence graph. In the present analysis, the goal was to infer a network among genes, which corresponds to a sparse estimate of the precision matrix (74).

#### Other Statistical Analysis

Data are presented as means  $\pm$  1 SE except in Table 2, where the data are presented as means  $\pm$  SD. The significance of differences in mean values between and within the rat strains was evaluated by a two-way repeated-measure ANOVA for blood pressure and proteinuria data or a two-way ANOVA for the Western blot analysis, followed by a Holm-Sidak test for preplanned comparisons. A  $P < 0.05$  using a two-tailed test was considered statistically significant.

## RESULTS

### Blood Pressure and Proteinuria Before and Following 14 Days of HS Diet

Summarized in Fig. 1 are the blood pressure, HR, and albumin data measured on day 14 of HS diet for the SS and congenic SS.13<sup>BN26</sup> and the 13 overlapping subcongenic strains 26-A through 26-M spanning the 13.11 Mb region. MAP, systolic (SAP) and diastolic blood pressure (DAP), and HR are summarized as well as the albuminuria ( $U_{albV}$ ). Seven of the 13 overlapping subcongenic strains spanning the region from 80.92 to 82.29 Mb (1.37 Mb) were significantly protected ( $P < 0.05$ ) by  $>26$  mmHg from the development of hypertension compared with the SS. This included strains 26-E, 26-F,

26-G, 26-J, 26-K, 26-L, and 26-M. MAP of the other six strains did not differ significantly from SS rats. This led to the identification of the 1.37 Mbp region on chr 13 containing genes that influenced MAP of the SS rats on an HS diet. The index of renal injury,  $U_{albV}$ , paralleled these distinctions in MAP as summarized in this figure.

Both SAP and DAP values tracked the MAP in each of the strains, thereby mapping to the same region of chr 13. There was little correlation between HR and blood pressures between strains, indicating that HR is independently determined.

### Genomic DNA Sequencing of the Candidate Region

DNA sequencing was carried out to fill the genomic gaps within the congenic SS.13<sup>BN26</sup> region (13.11 Mbp) and to enable identification of genes in the narrow 1.37 Mbp subcongenic region. As shown in Fig. 2, from the initial 78 sequence gaps in the region on the reference genome, we have reduced the number to only 19 gaps within this 1.37 Mbp region representing  $<1\%$  of the sequence of this region. The size of these remaining gaps is detailed in Table 2. Based on this completed sequence, five genes were found to reside in the 1.37 Mbp subcongenic region: *Rfwd2*, *Astn1*, *Fam5b*, *Pappa2*, and *Tnr* as shown.

Since the exact same rat that provided the reference sequence for Rn5BN was used for these high-coverage BAC sequences, these data also enabled an error correction of the reference genome. Specifically, 100 nucleotides [e.g., false single nucleotide polymorphisms (SNPs)] were corrected in the 1.37 Mbp region for the BN sequence. The SS rat sequence,

Table 2. The details of the 19 remaining gaps in the 1.37 Mp region

Gap	Chromosome	Start	End	Size, bp
1	CHR13	81002976	81003754	775
2	CHR13	81205434	81206282	847
3	CHR13	81313716	81319472	5756
4	CHR13	81346053	81352174	6121
5	CHR13	81436686	81442206	5520
6	CHR13	81450713	81453080	2367
7	CHR13	81512283	81513253	970
8	CHR13	81532453	81533962	1509
9	CHR13	81574610	81576054	1444
10	CHR13	81663495	81664431	934
11	CHR13	81689446	81693383	3937
12	CHR13	81776602	81777422	820
13	CHR13	81791857	81793835	1978
14	CHR13	81906842	81908331	1489
15	CHR13	81915421	81923258	7837
16	CHR13	81950585	81953290	2705
17	CHR13	81972548	81973328	780
18	CHR13	82105934	82107034	1100
19	CHR13	82285410	82286743	1333

Table 3. The SS rat sequence, determined by the Illumina system, compared with the Rn5BN reference sequence obtained from the BN rat and annotated with ANNOVAR

SNP Type	n (ANNOVAR)
Downstream	3
Intergenic	1,368
Intronic	637
Synonymous coding	4
Upstream	2
UTR3	11
Total	2,025

Shown in this Table are various types and numbers of sequence variants found within the 1.37 Mbp subcongenic region of interest between the SS and BN strains.

determined using the Illumina system, was compared with the Rn5BN reference sequence obtained from the BN rat, and variants were annotated using ANNOVAR. As summarized in Table 3, within the 1.37 Mbp subcongenic region of interest 2,025 sequence variants were found between the SS and BN strains, of which three were downstream of genes (1 kb from transcription end), 1,368 were intergenic, 637 intronic, four were synonymous coding variants, two upstream of genes (1 kb from start site), and 11 in 3'-untranslated region. None of these SNPs were located in transcription factor binding sites. Detailed analysis of the genomic sequence of Rfwd2 revealed 75 SNPs residing in intronic regions. None of these SNPs was located in the 10 bp region of the donor or acceptor sites. However, we cannot exclude the possibility that some intronic SNPs could influence the expression of isoforms such as those found for Rfwd2 shown in Fig. 3.

#### RNA Expression

Each of the five genes in the 1.37 Mb region shown in Fig. 2 (*Rfwd2*, *Astn1*, *Fam5b*, *Pappa2*, and *Tnr*) was measured in the RNA-seq analysis, and each was also represented on the GeneChip. However, only three of the genes were quantifiable by rt-PCR in the renal outer medulla: *Rfwd2*, *Astn1*, and *Fam5b*. *Rfwd2* was found to be the most highly expressed of these genes in this region in the outer medulla and exhibited multiple splice variants by RNA-seq analysis.

#### Western Blot Analysis

Rfwd2 protein levels from outer medulla were examined by Western blot in the salt-sensitive SS compared with the subcongenic salt-resistant 26-M, which displayed the minimal subcongenic region containing *Rfwd2* (and *Astn1*, *Fam5b*, *Pappa2*, *Tnr*). This strain was selected to minimize the likelihood of epistatic interactions beyond that region that could occur when comparing to other subcongenic strains. Two of the Rfwd2 isoforms identified by RNA-seq analysis predicted the size of two proteins detected by the antibody for Rfwd2; a 75 kDa band (*band 1*), corresponding to the longer isoform, and a ~50 kDa band (*band 3*) corresponding to the shorter isoform. As shown in Fig. 3, the larger protein of *band 1* was found to be expressed at higher levels in the SS on both 0.4 and 8% salt diet compared with the 26-M strain and was significantly higher in the SS on 0.4% than 8% salt diet. The lower-molecular-weight protein of *band 3*, was present at similar levels in both salt-sensitive SS and the salt-resistant

26-M when fed the LS diet (0.4%). However, the HS diet (8%) resulted in a significant increase only in the SS strain, which was higher than the 26-M strain ( $P < 0.05$ ). Comparisons carried out in several other strains generally indicated a consistent relationship of the shorter isoform (*band 3*) of protein expression with increased blood pressure. This was the case when SS (salt-sensitive) was compared with the SS.13<sup>BN26</sup> (salt-resistant) strain, and 26-I (salt-sensitive) compared with the 26-J (salt-resistant) strain.

#### Bayesian Analyses

The normalized and merged gene expression data yielded a high level of correlation in RNA-seq data with our Affymetrix GeneChip data previously published (43) with an  $r = 0.89$  for SS rats and  $r = 0.89$  for SS.13<sup>BN26</sup> rats (Fig. 4). The Bayesian model analysis (65) incorporating all 243 KEGG biological pathways identified seven pathways with the greatest likelihood (i.e., highest posterior probabilities) to distinguish blood pressure levels among experimental groups (Table 4). The seven pathways are #04080 (neuroactive ligand-receptor interaction) followed by #00400 (phenylalanine, tyrosine and tryptophan biosynthesis), #00460 (cyanoamino acid metabolism), #03450 (nonhomologous end-joining), #04122 (sulfur relay

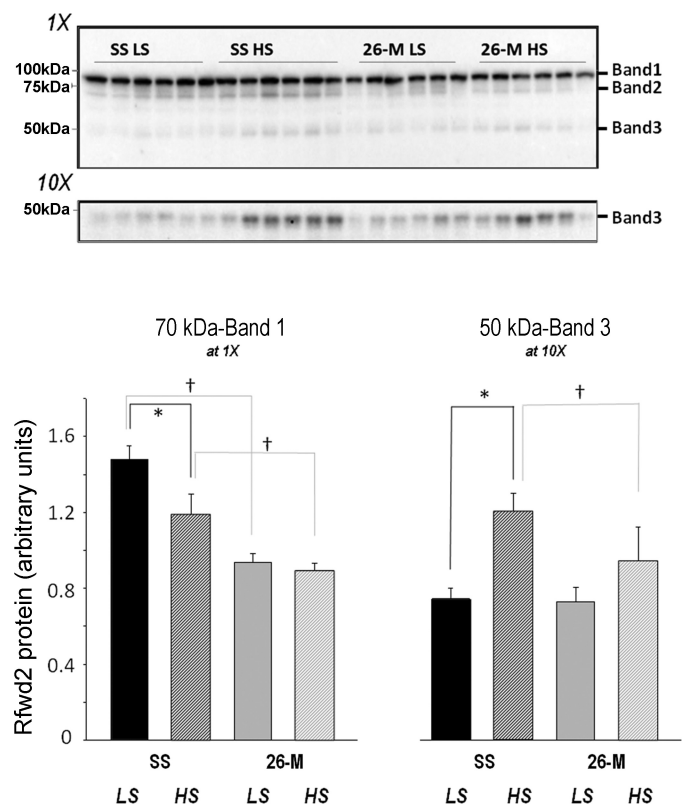


Fig. 3. Western blot analysis of Rfwd2 expression in renal outer medullary tissue collected from salt-sensitive SS and the salt-resistant subcongenic strain 26-M fed either 0.4% NaCl [low salt (LS)] or 8% NaCl for 7 days (HS). Two distinct bands were quantified corresponding to 70 kDa (*band 1*) and 50 kDa (*band 3*) on the gel shown. *Band 1* was quantified at 1X, while *band 3* was quantified at 10X as shown. The intensity was normalized to the corresponding lane intensity for Coomassie blue-stained membrane for each band. The results of the analysis of the abundance of the Rfwd2 protein are shown in the bottom panel. \*Significant difference between LS and HS conditions within the strain ( $P < 0.5$ ). †Significant difference between strains ( $P < 0.05$ ).

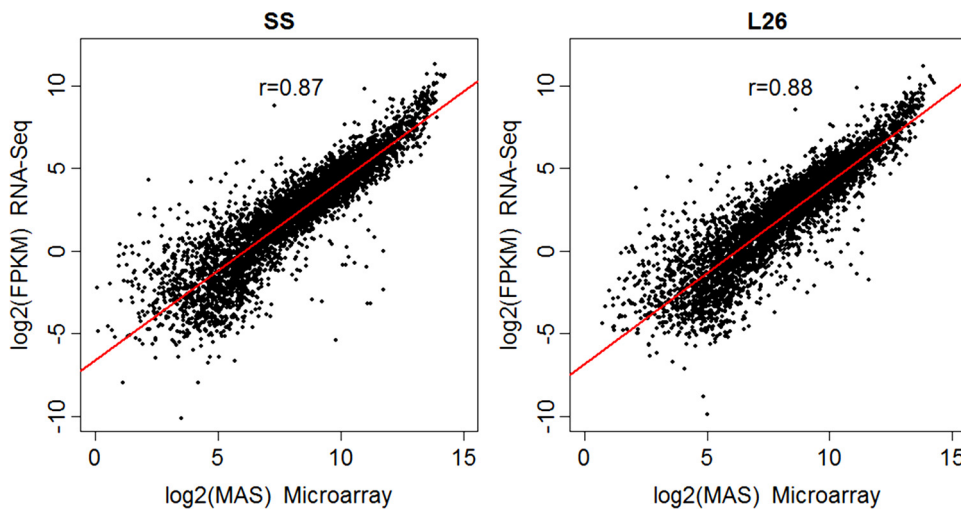


Fig. 4. Correlations between gene expression data determined by Affymetrix GeneChip (microarray) and RNA-seq are summarized. Separate comparisons of SS (left) and SS.13<sup>BN26</sup> (right) rats were made. To determine these correlations, three replicates were combined for the RNA-seq data [fragments per kilobase of exon per million fragments mapped (FPKM) = 0 values were not included, and expression represented by multiple probes for individual genes were averaged].

system), #04610 (Complement and coagulation cascades including 3 subpathways: kallikrein kinin, complement cascade, and coagulation cascade), and #04950 (maturity onset diabetes of the young).

These pathways, together with others selected based on their known relevance to blood pressure regulation (see Table 5), were then used to infer relationships among genes *Rfwd2*, *Astn1*, and *Fam5b* and other genes within the pathways using the GGM (74). Only these three genes in the 1.37 Mbp region exhibited quantifiable amounts of RNA expression levels in the renal outer medulla. The resulting inferred pathways are collectively shown in Fig. 5, where the nodes denote genes while the edges indicate the interdependence (e.g., conditional dependence) between the expression levels of two genes. The edges were chosen using the criterion that the posterior probability of edge inclusion was at least 0.5. It is important to recognize that these graphical inference models do not necessarily reflect regulatory relationships between genes depicted in typical biological pathways. Instead, the inferred graphical models reflect the likelihood of some type of interdependence of these genes among each other. A complete table of these associations is found in Supplemental Table S1a–S1s.<sup>1</sup>

The genes found to be highly correlated with one or more of the three candidate genes (*Rfwd2*, *Astn1*, and *Fam5b*) and within more than one KEGG pathway are summarized in Table 6.

<sup>1</sup> The online version of this article contains supplemental material.

Table 4. Pathways most likely to distinguish blood pressure levels among experimental groups based on the Bayesian model analysis

KEGG Pathway Number	KEGG Pathway Name	Posterior Probability
04080	neuroactive ligand-receptor interaction	0.784
00400	phenylalanine, tyrosine, and tryptophan biosynthesis	0.565
00460	cyanoamino acid metabolism	0.555
03450	nonhomologous end-joining	0.432
04122	sulfur relay system	0.423
04610	complement and coagulation cascades	0.402
04950	maturity onset diabetes of the young	0.401

The KEGG pathway numbers or names of biological subpathways containing these genes are listed together with the number of pathways in which an edge exists to each of the three candidate genes. It is seen that *Rfwd2* exhibits the greatest number of edges with the genes in the pathways of interest. The results provide unique insights as to whether the relationship between two genes could be explained by other genes present in the pathway being analyzed. For example, *Mdh1* was present in two pathways analyzed and showed an edge with *Rfwd2* in both pathways, suggesting that the correlation between *Mdh1* and *Rfwd2* could not be explained by other genes present in either of the two pathways. In contrast, *Hsd11b2* was also present in two pathways analyzed but showed an edge with *Rfwd2* in only one of the two pathways, suggesting that the correlation between *Rfwd2* and *Hsd11b2* could not be explained by genes present in the pathway that showed an edge between *Rfwd2* and *Hsd11b2* but could be explained by genes present in the pathway that did not show an edge between the two genes.

We achieved a level of confirmation in these model predictions when using the GeneChip data from rats described in Table 1. It was found that of the seven genes showing association with *Rfwd2* in Table 6, the mRNA of four of these genes was expressed in different amounts ( $P < 0.05$ ) in SS compared with congenic SS.13<sup>BN26</sup> rats. These include *ATP1b2*, lower in SS rats fed HS; *Mdh1*, higher in SS rats fed LS and reduced by the HS diet; *Pck2*, lower in SS rats fed either LS or HS diet; *Serpine1* (extracellular), higher in SS rats fed HS.

Table 7 focuses on genes showing average partial correlation  $> 0.2$  with at least one of the three genes in the region. It is seen that *Rfwd2* is positively correlated with eight genes in six pathways [*F8* (Factor VIII), *Csnk1d*, *Pik3ca*, *Adsl*, *Btrc*, *Vipr2*, *Acly*, and *Clock*] and negatively correlated to one gene (*Cyp11a1*) in one pathway. Again using the GeneChip data from rats described in Table 1, we found five of the nine genes that were highly correlated with *Rfwd2* to be significantly different ( $P < 0.05$ ) comparing the renal medullary tissue of the SS and salt-insensitive SS.13<sup>BN26</sup> rats. These included *F8* (lower in SS rats fed either LS or HS); *Csnk1d* (higher in SS rats fed either LS or HS); *Pik3ca* (lower in SS rats fed LS and suppressed in both strains fed an HS diet); *Adsl* (lower in SS rats fed LS or HS); and *Acly* (increased with HS

Table 5. KEGG pathways analyzed by the Bayesian graphical model analysis

KEGG Pathway Number	KEGG Pathway Name	Genes in KEGG Pathway, <i>n</i>	Genes in Dataset, <i>n</i>
<i>Pathways selected with known relevance in blood pressure regulation</i>			
0020	citrate cycle (TCA cycle)	30	23
00140	steroid hormone biosynthesis	56	20
00250	alanine, aspartate, and glutamate metabolism	32	21
00910	nitrogen metabolism	23	7
04614	renin-angiotensin system	16	12
04710	circadian rhythm-mammal	23	17
04960	aldosterone-regulated sodium reabsorption	42	24
04961	endocrine and other factor-regulated calcium reabsorption	48	31
04964	proximal tubule bicarbonate reclamation	22	15
04966	collecting duct acid secretion	27	17
<i>Pathways selected with posterior probability &gt; 0.4 (see METHODS)</i>			
04080	neuroactive ligand-receptor interaction	272	subset of 32
00400	phenylalanine, tyrosine, and tryptophan biosynthesis	5	4
00460	cyanoamino acid metabolism (also selected above)	7	5
03450	nonhomologous end-joining	13	6
04122	sulfur relay system	10	7
04610	complement and coagulation cascades (subpathways: kallikrien, complement, and coagulation)	69	11, 10, 17
04950	maturity onset diabetes of the young	24	20

in both strains). *Cy11a1*, *Vipr2*, and *Clock* were not detectable by microarray (43).

Also shown in Table 7, *Astm1* was positively correlated with three genes and negatively correlated with another three genes within nine different pathways of interest. Finally, *Fam5b* exhibited a high partial correlation with only a single gene, *Cpb2*.

## DISCUSSION

The present study had two goals. First, to narrow a region of chr 13 by exclusion mapping to one region containing a small number of genes that could singularly or epistatically modify blood-pressure salt sensitivity. Second, to apply unbiased statistical approaches to identify molecular networks and biological pathways associated with the genes within this region to provide insights on how these genes could reverberate through the biological system to modify blood-pressure salt sensitivity.

The first goal was achieved as we extended our efforts to map genes of relevance to salt sensitivity in the SS rat utilizing chromosomal substitution approaches (10, 14, 21, 28, 39, 48, 52, 54). We have previously reported four nonoverlapping regions within chr 13 in which substitution of BN alleles provided protection from hypertension in SS rats (52). One of these regions was a 13.11 Mbp segment of the BN rat chr 13 (from position 73.37 to 86.48 Mbp), which, when introgressed into chr 13 of the SS rat, significantly attenuated salt-induced hypertension (congenic strain SS.13<sup>BN26</sup>). In the present study, this congenic inbred strain was backcrossed to the SS strain to further narrow the region and identify genes of interest by developing multiple overlapping subcongenic strains. By exclusion mapping, this resulted in a 1.37 Mbp region on chr 13 (positions 80.92 to 82.29 Mbp) within which we identified five genes: *Rfwd2*, *Fam5b*, *Astm1*, *Pappa2*, and *Tnr*. None of these genes are currently known to be involved in hypertension.

Among these genes, *Rfwd2* was expressed at higher levels within the renal medulla than the other four candidate genes.

Since *Rfwd2* was found to be most strongly associated with the pathways involved in blood pressure regulation, most of our discussion will focus on this gene. *Rfwd2* has no known cardiovascular-related functions. An evolutionarily conserved E3 ubiquitin ligase (also known as COP1), *Rfwd2* in mammals functions as a FoxO1 ubiquitin E3 ligase to regulate FoxO1-mediated gene expression (32). It acts as a tumor suppressor by inducing p53 degradation and promoting the destruction of c-JUN (50), thereby promoting cell cycle progression and cell survival. Deficiency of *Rfwd2* leads to spontaneous tumor formation in mice (46). In its capacity as a ubiquitin ligase, *Rfwd2* promotes acetyl-coenzyme A ubiquitination by utilizing TRB3 as an adaptor protein and has been linked to fat metabolism during fasting (56). Interestingly, *Rfwd2* has been found to interact with *Trib 1* (62), which is critical for the differentiation of proinflammatory F4/80(+)MR(+) tissue-resident macrophages, potentially connecting it to tissue remodeling and fibrosis seen in the outer medulla of the SS rat (48). This is of relevance given the recent studies by De Miguel and associates (12), showing the important role that renal infiltration of lymphocytes plays in the development of hypertension and renal fibrosis in SS rats.

*Fam5b* (BMP/retinoic acid-inducible neural-specific protein 2, also known as BRINP2) is expressed largely in the central and peripheral nervous system and is thought to play a role in cell cycle regulation during the development and maintenance of the nervous system (33, 70). No mutant or knockout data are currently available. *Astm1* (neuronal protein astrotactin) is a well-studied receptor for glial-guided neuronal migration (1, 16, 20, 79) and has been implicated in several common disorders of the nervous system (attention deficit hyperactivity disorder, autism, and schizophrenia) (22, 26, 30, 40, 73). *Pappa2* encodes a member of the pappalysin family of metzincin metalloproteinases that cleaves insulin-like growth factor-binding protein 5 and is thought to be a local regulator of insulin-like growth factor bioavailability (8). *Tnr* (tenascin-R)

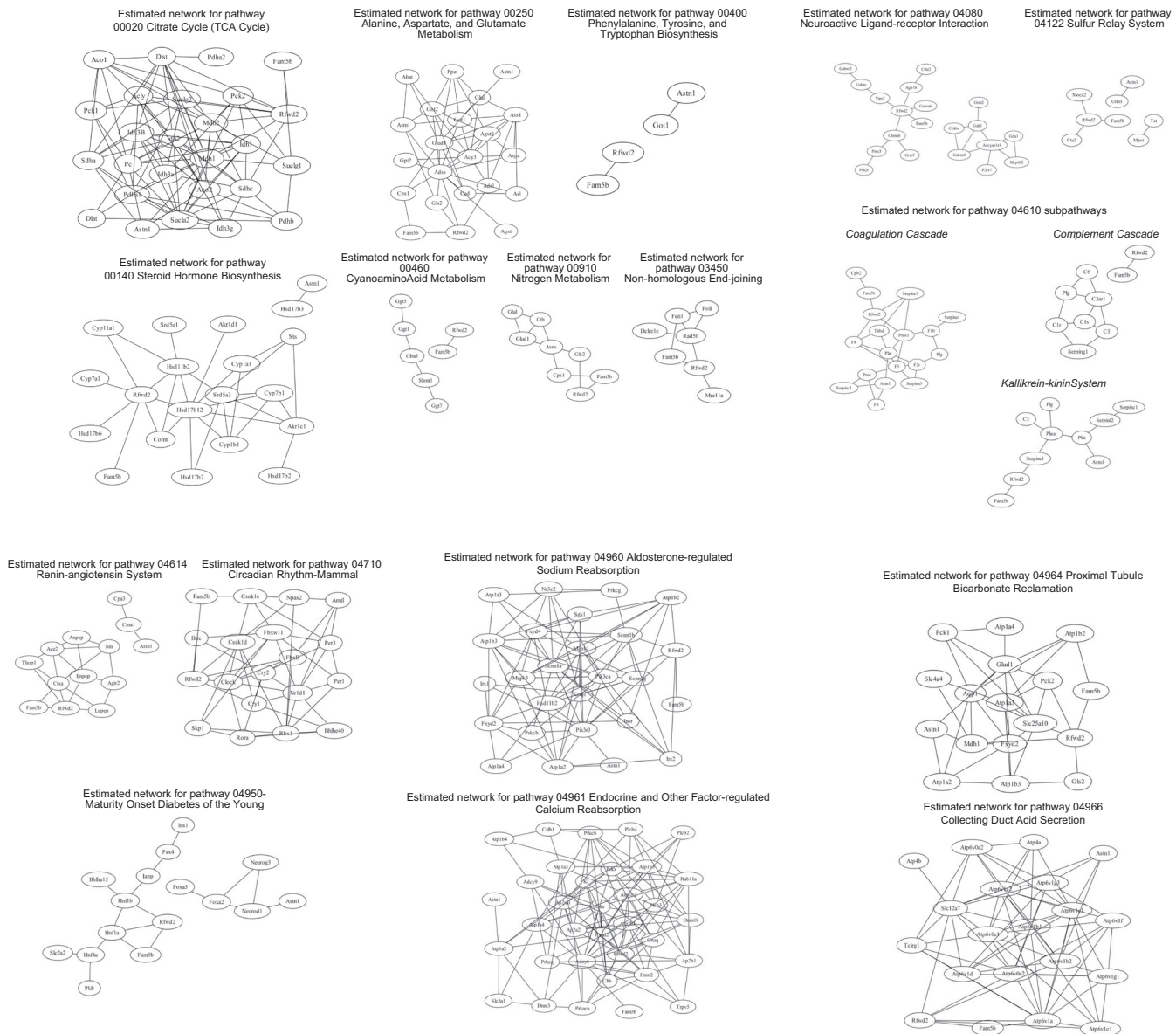


Fig. 5. Bayesian graphical model is depicted for each of the 19 KEGG pathways analyzed (listed in Table 4). Each schematic displays the connections of the 3 candidate genes, *Rfwd2*, *Astm1*, and *Fam5b*, located in the 1.37 Mbp region, with other genes in the pathway.

is an extracellular matrix glycoprotein expressed primarily in the central nervous system (11).

*Bayesian Analysis of Pathways and Genes*

Given the well-recognized polygenic and multifactorial nature of hypertension in the SS rat (10, 57) it is evident that a single allelic variation will not explain this complex form of hypertension. Application of the recently developed Bayesian modeling approaches used in this study yielded novel and interesting clues regarding mechanisms and pathways, whereby several of the genes in our defined region of interest are likely to participate in this SS form of hypertension. As none of the genes within the narrow congenic region are known to be involved in hypertension, this unbiased Bayesian modeling has provided useful clues to be experimentally explored.

*Genes exhibiting high levels of interdependence with Rfwd2 in multiple pathways.* Of the genes that were found to be highly correlated with *Rfwd2* within more than one KEGG pathway (Table 6) at the top of the list were *Atp1b2* (Na, K-ATPase family) and *Fxyd2*, a gamma subunit of Na, K-ATPase. *Atp1b2* mRNA expression was found to be significantly higher in the renal medulla of SS.13<sup>BN26</sup> compared with SS rats on both LS and HS diets. Both *Atp1b2* and *Fxyd2* were prominent in three different KEGG pathways, #04960 (Aldosterone-regulated Na<sup>+</sup> reabsorption), #04961 (Endocrine and other factor-regulated Ca<sup>2+</sup> reabsorption), and #04964 (Proximal tubule bicarbonate reclamation). *Rfwd2* was also highly correlated with *Hsd11b2* (11-beta-dehydrogenase type II), an isozyme that catalyzes the glucocorticoid cortisol conversion to the inactive metabolite cortisone, thereby preventing illicit activation of the

Table 6. Genes found to be highly correlated with 1 or more of the 3 candidate genes (*Rfwd2*, *Astn1*, and *Fam5b*) within > 1 KEGG pathway

Gene Name	KEGG Pathway Number Including Gene	Pathways Including Gene, n	Edges to <i>Fam5b</i> , n	Edges to <i>Astn1</i> , n	Edges to <i>Rfwd2</i> , n
<i>Atp1a2</i>	04960, 04961, 04964	3	0/3	3/3	0/3
<i>Atp1b2</i>	04960, 04961, 04964	3	1/3	0/3	2/3
<i>Fxyd2</i>	04960, 04961, 04964	3	0/3	0/3	1/3
<i>Gls2</i>	00250, 00910, 04964	3	0/3	0/3	3/3
<i>Glud1</i>	00250, 00910, 04964	3	0/3	1/3	0/3
<i>Cps1</i>	00250, 00910	2	2/2	0/2	0/2
<i>Got1</i>	00250, 00400	2	0/2	2/2	0/2
<i>Hsd11b2</i>	00140, 04960	2	0/2	0/2	1/2
<i>Mdh1</i>	00020, 04964	2	0/2	2/2	2/2
<i>Pck2</i>	00020, 04964	2	0/2	0/2	2/2
<i>Plat</i>	coagulation cascade, kallikrien kinin system	2	0/2	2/2	0/2
<i>Serpinc1</i>	coagulation cascade, kallikrien kinin system	2	0/2	1/2	0/2
<i>Serpine1</i>	coagulation cascade, kallikrien kinin system	2	0/2	0/2	2/2

mineralocorticoid receptor known to be important in hypertension (47). Together, these relationships link *Rfwd2* to genes known to be of importance in establishing transcellular Na<sup>+</sup> and K<sup>+</sup> electrochemical gradients, in renal tubular Na<sup>+</sup> transport, and in hypertension.

Among the other genes highly correlated with *Rfwd2* were *Gls2*, *Mdh1*, and *Pck2*. The first of these (phosphate-activated glutaminase) resides in three pathways including #00250 (Alanine, aspartate, and glutamate metabolism), #00910 (nitrogen metabolism), and #04964 (Proximal tubule bicarbonate reclamation). *Gls2* encodes a mitochondrial phosphate-activated glutaminase that is induced in response to DNA damage or oxidative stress in a p53-dependent manner (67). *Mdh1* (malate dehydrogenase) was highly correlated with *Rfwd2* in two pathways, #00250 (Alanine, aspartate, and glutamate metabolism) and #04964 (Proximal tubular bicarbonate reclamation). It is known that *Mdh1* encodes an enzyme that catalyzes the reversible oxidation of malate to oxaloacetate in the citric acid cycle. Finally, *Pck2* is a gene known to encode a mitochondrial enzyme that catalyzes the conversion of oxaloacetate to phos-

phenolpyruvate in the citric acid cycle. The link of *Rfwd2* to TCA cycle and cell energetics was again implied by the high correlation with *Acly* (ATP citrate lyase; Table 7), which encodes the primary enzyme responsible for the formation of acetyl-CoA and oxaloacetate from citrate and CoA with a concomitant hydrolysis of ATP to ADP and phosphate. Together, these data suggest that *Rfwd2* could be an important causal gene responsible for observed differences in cellular energetics that we have described in the medullary thick ascending limb of the renal outer medulla (78).

Mitochondrial and metabolic deficiencies have emerged as a new mechanism contributing to the development of hypertension (41). In particular, fumarase, an enzyme in the tricarboxylic acid cycle, has been shown to be genetically altered and functionally insufficient in the renal medulla of SS rats compared with SS.13<sup>BN</sup> rats (71, 72). In a proteomic analysis of mitochondria obtained from the medullary thick ascending limb of SS rats, we have also found seven proteins to be differentially expressed between the salt-sensitive SS rat and the salt-resistant SS.13<sup>BN</sup> rat, which are integral enzymes in the TCA cycle. These observations

Table 7. Genes showing average partial correlation > 0.2 with at least 1 of the 3 genes in the region (e.g., probability of edge inclusion > 80%)

Gene Name	KEGG Pathway Number Including Gene	Average Abs Partial Correlation With	Sign of Partial Correlation
<b><i>Rfwd2</i>:</b>			
<i>F8</i>	coagulation cascade	0.309	+
<i>Csmk1d</i>	04710	0.290	+
<i>Pik3ca</i>	04960	0.259	+
<i>Cyp11a1</i>	00140	0.221	-
<i>Adsl</i>	00250	0.218	+
<i>Btrc</i>	04710	0.216	+
<i>Vipr2</i>	04800	0.213	+
<i>Acly</i>	00020	0.204	+
<i>Clock</i>	04710	0.203	+
<b><i>Astn1</i>:</b>			
<i>Atp1a2</i>	04960, 04961, 04964	0.267	-
<i>F5</i>	coagulation cascade	0.261	+
<i>Atp6v1e1</i>	04966	0.251	+
<i>Urm1</i>	04122	0.249	-
<i>Neurod1</i>	04950	0.218	-
<i>Got1</i>	00250, 00400	0.205	+
<b><i>Fam5b</i>:</b>			
<i>Cpb2</i>	coagulation cascade	0.318	+

are consistent with observed reductions in efficiency of oxygen utilization and excess generation of reactive oxygen species in the medulla of the SS rat (78).

*Genes exhibiting high levels of partial correlation with Rfwd2.* A strong correlation of *Rfwd2* with *F8* (Factor VIII) was found (Table 7) and also a high level of interdependence with *Serpine 1* (Table 6), which encodes antithrombin in the coagulation cascade pathway. The mRNA expression of both of these genes was found to be differentially expressed in the renal medulla of SS compared with SS.13<sup>BN26</sup> rats fed an HS diet. Although interesting, it is unclear how this would affect renal function and arterial blood pressure. *Rfwd2* was also correlated with *Pik3ca*, *Cyp11a1*, and *Adsl* (Table 7). The first of these, *Pik3ca*, is a member of the broad family of phosphatidylinositol 3-kinases, which has a diverse set of cellular functions including cell growth, proliferation, differentiation, motility, survival, and intracellular trafficking, which could influence metabolic processes and blood pressure in many ways. The mRNA expression of this gene was significantly higher in the salt-resistant SS.13<sup>BN26</sup> compared with SS rats. *Cyp11a1* (cholesterol side-chain cleavage enzyme) catalyzes the conversion of cholesterol to pregnenolone and is the first and rate-limiting step in steroid hormone synthesis. *Adsl* is involved in synthesis of purines and formation of adenosine monophosphate from inosine monophosphate.

*Circadian rhythm pathway.* One of the most interesting and unpredicted outcomes of our analysis was the high correlation of *Rfwd2* with a number of genes that interact with the circadian rhythm pathway (Table 7). *Rfwd2* as an E3 ubiquitin ligase is known to be critically involved in the stabilization of PERIOD2, an essential component of the mammalian circadian oscillator (58). *Btrc* (F-box/WD repeat-containing protein 1A) is one of the four subunits of the E3 ubiquitin protein ligase complex and known to participate in the circadian stabilization process (58). *Csnk1d* (casein kinase I isoform delta) is also a member of the clock gene family and acts as a serine/threonine protein kinase that phosphorylates core clock proteins of the mammalian circadian oscillator (18, 38). *Vipr2* (vasoactive intestinal peptide receptor 2) has also been implicated in circadian rhythms (24) and basal energy expenditure (2). Finally, *Clock* (circadian locomotor output cycles Kaput), which functions as an essential activator of downstream elements in circadian rhythm pathway, was also found to be highly correlated with *Rfwd2*.

Circadian rhythms exert powerful effects on metabolic cycles that, when interrupted, can directly and indirectly affect cardiovascular functions (36). There is evidence that derangements of circadian clock-controlled mechanisms can contribute to the onset and maintenance of hypertension (60). The mechanism of synchronization between the central and clock ma-

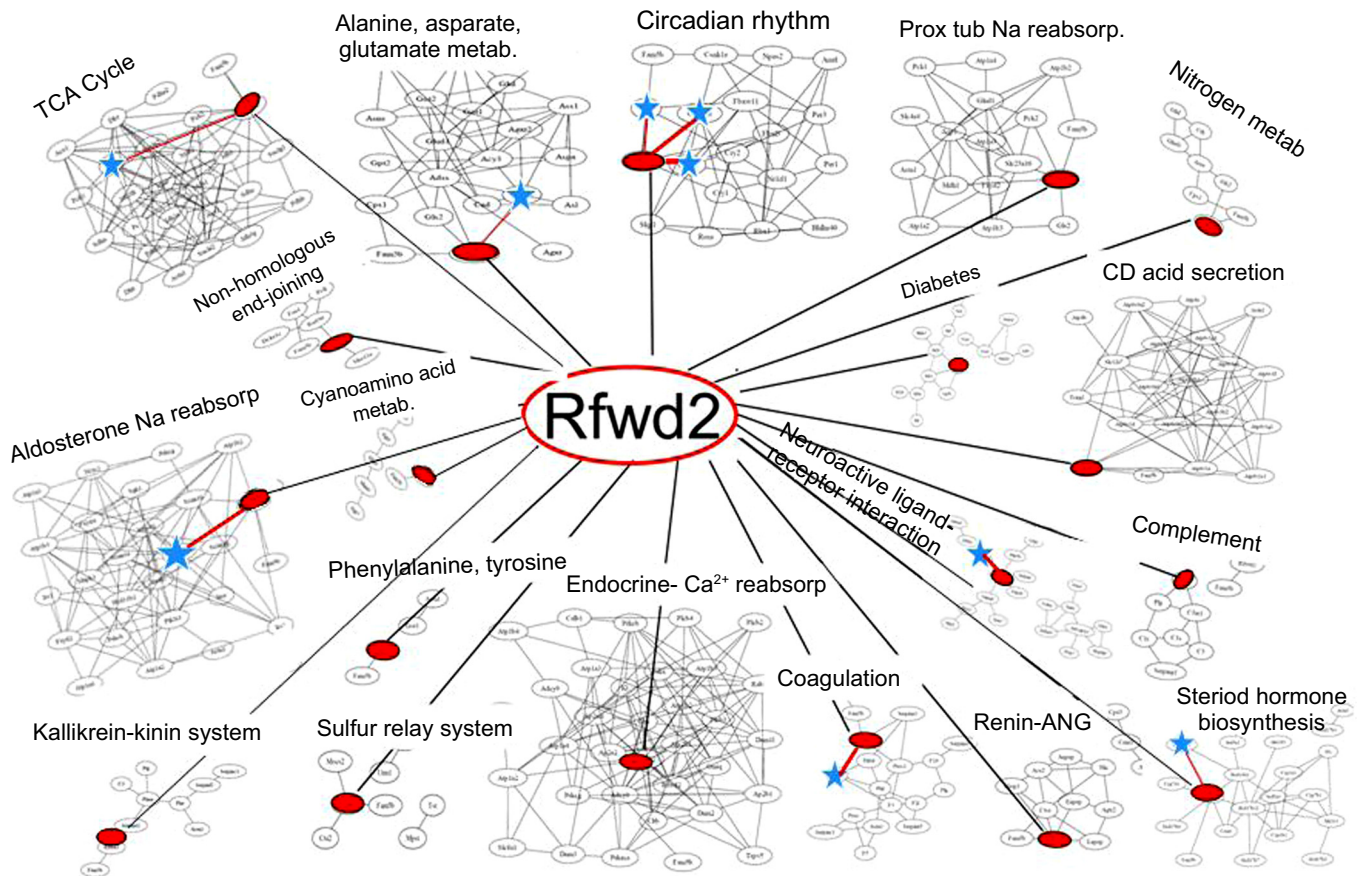


Fig. 6. Schematic summary of inferred Bayesian networks of the 19 pathways focusing on the relationship of *Rfwd2* and those genes that exhibited the highest-ranked partial correlations with *Rfwd2*. The red-filled ellipses within each pathway represent the *Rfwd2* node (denoting gene expression levels). The blue stars represent those genes listed in Table 7 that exhibited partial correlations >0.2 for *Rfwd2* with the red lines representing the edges (interdependence) between *Rfwd2* and these starred genes.

chinery of the kidney are only now beginning to be studied with renal phenotypes being explored in mutant rodent models (5). It has been found that aldosterone mediates an increase in *Per1* through a DNA/mineralocorticoid receptor interaction that in turn regulates the alpha subunit of the renal epithelial sodium channel ( $\alpha$ -ENaC) in renal collecting ducts (59). It is relevant that in patients with SS hypertension or chronic kidney disease the typical fall of night-time blood pressure is frequently lost, the so-called “nondipper” pattern, and is associated with nocturnal hypertension, a risk factor for cardiovascular events (25, 35). The relationships found in the present study indicate that *Rfwd2* could be importantly involved in the regulation of renal circadian events and thereby affect the regulation of blood pressure in SS rats.

### Summary

The present study utilized 13 overlapping congenic strains and identified by exclusion mapping a 1.37 Mbp region on chr 13 (positions 80.92 to 82.29 Mbp in the Rn5 genome assembly) that significantly influences the MAP in SS rats fed an HS diet. After DNA sequencing to fill gaps in the reference sequence in this region, five genes were identified (*Rfwd2*, *Astn1*, *Fam5b*, *Pappa2*, and *Tnr*). Of these five genes, *Rfwd2* was the most strongly expressed in the renal outer medulla. The Bayesian analyses indicated several genes that may connect *Rfwd2* to pathways related to blood pressure. As summarized in the schematic in Fig. 6, nine genes in the 19 blood pressure-related pathways exhibited very high partial correlations with *Rfwd2*. Four of these genes that were interdependent with *Rfwd2* exhibited significant differences in mRNA abundance between SS and salt-resistant congenic rats. Plausible mediators linking *Rfwd2* to mechanisms of arterial blood pressure regulation as indicated by partial correlation values include: 1) transcellular  $\text{Na}^+$  and  $\text{K}^+$  electrochemical gradients and tubular  $\text{Na}^+$  transport in the renal outer medulla; 2) the TCA cycle, cell energy production, oxidative stress; and 3) circadian rhythms. The study demonstrates a new, unbiased approach for identifying biological pathways mediating the effect of a candidate genomic region on hypertension.

### ACKNOWLEDGMENTS

Jenifer Phillips, Lisa Henderson, and Camille Taylor of the Biochemical Core Laboratory for measurement of albumin; gift of antibody for COP1 from Genentech, San Francisco, CA.

### GRANTS

PO1 HL-82798 (A. W. Cowley, Jr.); National Institutes of Health (NIH)/National Cancer Institute (NCI) T32 PreDoctoral Training Program in Biostatistics for Cancer Research (NCI T32 CA-096520) and by a training fellowship from the Keck Center of the Gulf Coast Consortia, on the National Library of Medicine (NLM) Training Program in Biomedical Informatics, NLM T15LM-007093 (C. B. Peterson); Cancer Center Support Grant (NCI Grant P30 CA-016672)(F. C. Stingo).

### DISCLOSURES

No conflicts of interest, financial or otherwise, are declared by the author(s).

### AUTHOR CONTRIBUTIONS

Author contributions: A.W.C., C.M., H.J.J., M.V., P.W.L., and M.L. conception and design of research; A.W.C., C.M., C.B.P., F.C.S., K.W.A., P.L., J.L., C.Y., T.K., and M.L. performed experiments; A.W.C., C.M., H.J.J., C.B.P., F.C.S., K.W.A., P.L., M.V., P.W.L., P.R., J.L., L.E., C.Y., T.K., and M.L. analyzed data; A.W.C., C.M., H.J.J., C.B.P., F.C.S., K.W.A., P.L., M.V.,

P.W.L., J.L., C.Y., and M.L. interpreted results of experiments; A.W.C., C.M., C.B.P., F.C.S., K.W.A., P.L., J.L., C.Y., and M.L. prepared figures; A.W.C., M.V., P.W.L., and M.L. drafted manuscript; A.W.C., C.M., C.B.P., F.C.S., K.W.A., P.L., M.V., P.W.L., J.L., L.E., C.Y., and M.L. edited and revised manuscript; A.W.C., C.M., H.J.J., C.B.P., F.C.S., K.W.A., P.L., M.V., P.W.L., P.R., J.L., L.E., C.Y., T.K., and M.L. approved final version of manuscript.

### REFERENCES

- Adams NC, Tomoda T, Cooper M, Dietz G, Hatten ME. Mice that lack astrotactin have slowed neuronal migration. *Development* 129: 965–972, 2002.
- Asnicar MA, Koster A, Heiman ML, Tinsley F, Smith DP, Galbreath E, Fox N, Ma YL, Blum WF, Hsiung HM. Vasoactive intestinal polypeptide/pituitary adenylate cyclase-activating peptide receptor 2 deficiency in mice results in growth retardation and increased basal metabolic rate. *Endocrinology* 143: 3994–4006, 2002.
- Atanur SS, Diaz AG, Maratou K, Sarkis A, Rotival M, Game L, Tschannen MR, Kaisaki PJ, Otto GW, Ma MC, Keane TM, Hummel O, Saar K, Chen W, Guryev V, Gopalakrishnan K, Garrett MR, Joe B, Citterio L, Bianchi G, McBride M, Dominiczak A, Adams DJ, Serikawa T, Flicek P, Cuppen E, Hubner N, Petretto E, Gauguier D, Kwitek A, Jacob H, Aitman TJ. Genome sequencing reveals loci under artificial selection that underlie disease phenotypes in the laboratory rat. *Cell* 154: 691–703, 2013.
- Aviv A, Hollenberg NK, Weder A. Urinary potassium excretion and sodium sensitivity in blacks. *Hypertension* 43: 707–713, 2004.
- Bonny O, Vinciguerra M, Gumz ML, Mazzocchi G. Molecular bases of circadian rhythmicity in renal physiology and pathology. *Nephrol Dial Transplant* 28: 2421–2431, 2013.
- Campese VM. Salt-sensitivity in hypertension. *Hypertension* 23: 531–550, 1994.
- Chaisson MJ, Tesler G. Mapping single molecule sequencing reads using Basic Local Alignment with Successive Refinement (BLASR): theory and application. *BMC Bioinformatics* 13: 238, 2012.
- Christians JK, Hoefflich A, Keightley PD. PAPP2, an enzyme that cleaves an insulin-like growth-factor-binding protein, is a candidate gene for a quantitative trait locus affecting body size in mice. *Genetics* 173: 1547–1553, 2006.
- Cowley AW Jr. Renal medullary oxidative stress, pressure-natriuresis, and hypertension. *Hypertension* 52: 777–786, 2008.
- Cowley AW Jr. The genetic dissection of essential hypertension. *Nat Rev Genet* 7: 829–840, 2006.
- David LS, Schachner M, Saghatelian A. The extracellular matrix glycoprotein tenascin-R affects adult but not developmental neurogenesis in the olfactory bulb. *J Neurosci* 33: 10324–10339, 2013.
- De Miguel C, Das S, Lund H, Mattson DL. T lymphocytes mediate hypertension and kidney damage in Dahl salt-sensitive rats. *Am J Physiol Regul Integr Comp Physiol* 298: R1136–R1142, 2010.
- De Miguel C, Guo C, Lund H, Mattson DL. Infiltrating T lymphocytes in the kidney increase oxidative stress and participate in the development of hypertension and renal disease. *Am J Physiol Renal Physiol* 300: F734–F742, 2011.
- Deng AY, Nattel S, Shi Y, L'heureux N, Cardin S, Menard A, Roy J, Tardif JC. Distinct genomic replacements from Lewis correct diastolic dysfunction, attenuate hypertension, and reduce left ventricular hypertrophy in Dahl salt-sensitive rats. *J Hypertens* 26: 1935–1943, 2008.
- Dobra A, Hans C, Jones B, Nevins JR, Yao G, West M. Sparse graphical models for exploring gene expression data. *J Multivariate Anal* 90: 196–212, 2004.
- Edmondson JC, Liem RK, Juster JE, Hatten ME. Astrotactin: a novel neuronal cell surface antigen that mediates neuron-astroglial interactions in cerebellar microcultures. *J Cell Biol* 106: 505–517, 1988.
- Elliot P, Marmot M, Dyer A, Joossens J, Kesteloot H, Stamier R, Stamier J, Rose G. The INTERSALT study: main results, conclusions and some implications. *Clin Exp Hypertens* 11: 1025–1034, 1989.
- Etcheberry JP, Machida KK, Noton E, Constance CM, Dallmann R, Di Napoli MN, DeBruyne JP, Lambert CM, Yu EA, Reppert SM, Weaver DR. Casein kinase 1 delta regulates the pace of the mammalian circadian clock. *Mol Cell Biol* 29: 3853–3866, 2009.
- Feng D, Yang C, Geurts A, Kurth T, Liang M, Lazar J, Mattson DL, O'Connor PM, Cowley AW Jr. Increased expression of NADPH oxidase subunit p67phox in the renal medulla contributes to excess oxidative stress and salt-sensitive hypertension. *Cell Metab* 15: 1–8, 2012.

20. Fishell G, Hatten ME. Astrotactin provides a receptor system for CNS neuronal migration. *Development* 113: 755–765, 1991.
21. Garrett MR, Meng H, Rapp JP, Joe B. Locating a blood pressure quantitative trait locus within 117 kp on the rat genome: substitution mapping and renal expression analysis. *Hypertension* 45: 451–459, 2005.
22. Glessner JR, Wang K, Cai G, Korvatska O, Kim CE, Wood S, Zhang H, Estes A, Brune CW, Bradfield JP, Imielinski M, Frackelton EC, Reichert J, Crawford EL, Munson J, Sleiman PM, Chiavacci R, Annaiah K, Thomas K, Hou C, Glaberson W, Flory J, Otieno F, Garris M, Soorya L, Klei L, Piven J, Meyer KJ, Anagnostou E, Sakurai T, Game RM, Rudd DS, Zurawiecki D, McDougle CJ, Davis LK, Miller J, Posey DJ, Michaels S, Kolevzon A, Silverman JM, Bernier R, Levy SE, Schultz RT, Dawson G, Owley T, McMahon WM, Wassink TH, Sweeney JA, Nurnberger JI, Coon H, Sutcliffe JS, Minshew NJ, Grant SF, Bucan M, Cook EH, Buxbaum JD, Devlin B, Schellenberg GD, Hakonarson H. Autism genome-wide copy number variation reveals ubiquitin and neuronal genes. *Nature* 459: 569–573, 2009.
23. Grim CE, Wilson TW. Salt, slavery, survival. Physiological principles underlying the evolutionary hypotheses of salt-sensitive hypertension in Western hemisphere Blacks. In: *Pathophysiology of Hypertension in Blacks*, edited by Fray JCS, Coyle JVG. New York: Oxford University Press, 1993, p. 25–49.
24. Harmar AJ, Marston HM, Shen S, Spratt C, West KM, Sheward WJ, Morrison CF, Dorin JR, Piggins HD, Reubi JC, Kelly JS, Maywood ES, Hastings MH. The VPAC2 receptor is essential for circadian function in the mouse suprachiasmatic nuclei. *Cell* 109: 497–508, 2002.
25. Hermida RC, Ayala DE, Smolensky ML, Mojon A, Fernandez JR, Crespo JJ, Moya A, Rios MT, Portaluppi F. Chronotherapy improves blood pressure control and reduces vascular risk in CKD. *Nat Rev Nephrol* 9: 358–368, 2013.
26. Hill SY, Weeks DE, Jones BL, Zezza N, Stiffler S. ASTN1 and alcohol dependence: family-based association analysis in multiplex alcohol dependence families. *Am J Med Genet B Neuropsychiatr Genet* 159B: 445–455, 2012.
27. Hoffman MJ, Flister MJ, Nunez L, Xiao B, Greene AS, Jacob HJ, Moreno C. Female-specific hypertension loci on rat chromosome 13. *Hypertension* 62: 557–563, 2013.
28. Joe B, Garrett MR, Dene H, Rapp JP. Substitution mapping of a blood pressure quantitative trait locus to a 2.73 Mb region on rat chromosome 1. *J Hypertens* 21: 2077–2084, 2003.
29. Kaczorowski CC, Stodola TJ, Hoffmann BR, Prisco AR, Liu PY, Didier DN, Karcher JR, Liang M, Jacob HJ, Greene AS. Targeting the endothelial progenitor cell surface proteome to identify novel mechanisms that mediate angiogenic efficacy in a rodent model of vascular disease. *Physiol Genomics* 45: 999–1011, 2013.
30. Kahler AK, Djurovic S, Julle B, Jonsson EG, Agartz I, Hall H, Opjordsmoen S, Jakobsen KD, Hansen T, Melle I, Wege T, Steen VM, Andreassen OA. Association analysis of schizophrenia on 18 genes involved in neuronal migration: MDGA1 as a new susceptibility gene. *Am J Med Genet B Neuropsychiatr Genet*. 147B: 1089–1100, 2008.
31. Kaneshisa M, Goto S, Sato Y, Furumichi M, Tanabe M. KEGG for integration and interpretation of large-scale molecular data sets. *Nucleic Acids Res* 40: D109–D114, 2012.
32. Kato S, Ding J, Pisch E, Jhala US, Du K. COP1 functions as a FoxO1 ubiquitin E3 ligase to regulate FoxO1-mediated gene expression. *J Biol Chem* 283: 35464–35473, 2008.
33. Kawano H, Nakatani T, Mori T, Ueno S, Fukaya M, Abe A, Kobayashi M, Toda F, Watanabe M, Matsuoka I. Identification and characterization of novel developmentally regulated neural-specific proteins, BRINP family. *Mol Brain Res* 125: 60–75, 2004.
34. Kim NH, Lang IM. Risk factors for chronic thromboembolic pulmonary hypertension. *Eur Respir Rev* 21: 27–31, 2012.
35. Kimura G, Dohi Y, Fukuda M. Salt sensitivity and circadian rhythm of blood pressure: the keys to connect CKD with cardiovascular events. *Hypertens Res* 33: 515–520, 2010.
36. Kohsaka A, Waki H, Cui H, Gouranud SS, Maeda M. Integration of metabolic and cardiovascular diurnal rhythms by circadian clock. *Endocr J* 59: 447–456, 2012.
37. Kotchen TA, Cowley AW Jr, Frohlich ED. Salt in health and disease - a delicate balance. *N Engl J Med* 368: 1229–1237, 2013.
38. Lee H, Chen R, Lee Y, Yoo S, Lee C. Essential roles of CKIdelta and CKIepsilon in the mammalian circadian clock. *Proc Natl Acad Sci USA* 106: 21359–21364, 2009.
39. Lee SJ, Liu J, Westcott AM, Vieth JA, DeRaedt SJ, Yang S, Joe B, Cicila GT. Substitution mapping in Dahl rats identifies two distinct blood pressure quantitative trait loci within 1.12- and 125-mb intervals on chromosome 3. *Genetics* 74: 2203–2213, 2006.
40. Lesch KP, Timmesfeld N, Renner TJ, Halperin R, Roser C, Nguyen TT, Craig DW, Romanos J, Heine M, Meyer J, Freitag C, Warnke A, Romanos M, Schafer H, Walitza S, Reif A, Stephan DA, Jacob C. Molecular genetics of adult ADHD: converging evidence from genome-wide association and extended pedigree linkage studies. *J Neural Transm* 115: 1573–1583, 2008.
41. Liang M. Hypertension as a mitochondrial and metabolic disease. *Kidney Int* 80: 15–16, 2011.
42. Liu Y, Liu P, Yang C, Cowley AW Jr, Liang M. Base-resolution maps of 5-methylcytosine and 5-hydroxymethylcytosine in Dahl S rats: effect of salt and genomic sequence. *Hypertension* 63: 827–838, 2014.
43. Lu L, Li P, Yang C, Kurth T, Misale M, Skelton M, Moreno C, Roman RJ, Greene AS, Jacob HJ, Lazar J, Liang M, Cowley AW Jr. Dynamic convergence and divergence of renal genomic and biological pathways in protection from Dahl salt-sensitive hypertension. *Physiol Genomics* 41: 63–70, 2010.
44. Lusher TF, Raij L, Vanhoutte PM. Endothelium-dependent vascular responses in normotensive and hypertensive Dahl rats. *Hypertension* 9: 157–163, 1987.
45. Maher B. Personal genomes: the case of the missing heritability. *Nature* 456: 18–21, 2008.
46. Marine JC. Spotlight on the role of COP1 in tumorigenesis. *Nat Rev Cancer* 12: 455–464, 2012.
47. Matsubara M, Kikuya M, Ohkubo T, Metoki H, Omori F, Fujiwara T, Suzuki M, Michimata M, Hozawa A, Katsuya T, Higaki J, Tsuji I, Araki T, Ogihara T, Satoh H, Hisamichi S, Nagai K, Kitaoka H, Imai Y. Aldosterone synthase gene (CYP11B2) C-334T polymorphism, ambulatory blood pressure and nocturnal decline in blood pressure in the general Japanese population: the Ohasama Study. *J Hypertens* 19: 2179–2184, 2001.
48. Mattson DL, Dwinell MR, Greene AS, Kwitek AE, Roman RJ, Jacob HJ, Cowley AW Jr. Chromosome substitution reveals the genetic basis of Dahl salt-sensitive hypertension and renal disease. *Am J Physiol Renal Physiol* 295: F837–F842, 2008.
49. Meng S, Roberts LJ 2nd, Cason GW, Curry TS, Manning RD Jr. Superoxide dismutase and oxidative stress in Dahl salt-sensitive and -resistant rats. *Am J Physiol Regul Integr Comp Physiol* 283: R732–R738, 2002.
50. Migliorini D, Bogaerts S, Defever D, Vyas R, Denecker G, Radaelli E, Zwolinska A, Depaepe V, Hocheppied T, Skarnes WC, Marine JC. Cop1 constitutively regulates c-Jun protein stability and functions as a tumor suppressor in mice. *J Clin Invest* 121: 1329–1343, 2011.
51. Miller JZ, Weinberger MH, Christian JC, Daugherty SA. Familial resemblance in the blood pressure response to sodium restriction. *Am J Epidemiol* 126: 822–830, 1987.
52. Moreno C, Kaldunski ML, Wang T, Roman RJ, Greene AS, Lazar J, Jacob HJ, Cowley AW Jr. Multiple blood pressure loci on rat chromosome 13 attenuate development of hypertension in the Dahl S hypertensive rat. *Physiol Genomics* 31: 228–235, 2007.
53. Moreno C, Kennedy K, Andrae JW, Jacob HJ. Genome-wide scanning with SSLPs in the rat. *Methods Mol Med* 108: 131–138, 2005.
54. Moreno C, Williams JM, Lu L, Liang M, Lazar J, Jacob HJ, Cowley AW Jr, Roman RJ. Narrowing a region of rat chromosome 13 that protects against hypertension in Dahl SS-13BN congenic strains. *Am J Physiol Heart Circ Physiol* 300: H1530–H1535, 2011.
55. Morrison J, Knoll K, Hessner MJ, Liang M. Effect of high glucose on gene expression in mesangial cells: upregulation of the thiol pathway is an adaptational response. *Physiol Genomics* 17: 271–282, 2004.
56. Qi L, Heredia JE, Altarejos JY, Sreaton R, Goebel N, Niessen S, Macleod IX, Liew CW, Kulkarni RN, Bain J, Newgard C, Nelson M, Evans RM, Yates J, Montminy M. TRB3 links the E3 ubiquitin ligase COP1 to lipid metabolism. *Science* 312: 1763–1766, 2006.
57. Rapp JP. Genetic analysis of inherited hypertension in the rat. *Physiol Rev* 80: 135–172, 2000.
58. Reischl S, Vanselow K, Westermark PL, Thierfelder N, Maier B, Herzel H, Kramer A. Beta-TrCP1-mediated degradation of PERIOD2 is essential for circadian dynamics. *J Bio Rhythms* 22: 375–386, 2007.
59. Richards J, Jeffers LA, All SC, Cheng KY, Gumz ML. Role of Per1 and the mineralocorticoid receptor in the coordinate regulation of  $\alpha$ ENaC in renal cortical collecting duct cells. *Front Physiol* 4: 253, 2013.

60. **Rudic RD, Fulton DJ.** Pressed for time: the circadian clock and hypertension. *Appl Physiol* 107: 1328–1338, 2009.
61. **Sanada H, Jones JE, Jose PA.** Genetics of salt-sensitive hypertension. *Curr Hypertens Rep* 13: 55–66, 2011.
62. **Satoh T, Kidoya H, Naito H, Yamamoto M, Takemura N, Nakagawa K, Yoshioka Y, Morii E, Takakura N, Takeuchi O, Akira S.** Critical role of Trib1 in differentiation of tissue-resident M2-like macrophages. *Nature* 495: 524–528, 2013.
63. **Schäfer J, Strimmer K.** An empirical Bayes approach to inferring large-scale gene association networks. *Bioinformatics* 21: 754–764, 2005.
64. **Shabalin AA, Tjelmeland H, Fan C, Perou CM, Nobel AB.** Merging two gene-expression studies via cross-platform normalization. *Bioinformatics* 24: 1154–1160, 2008.
65. **Stingo FC, Chen YA, Tadesse MG, Vannucci M.** Incorporating biological information into linear models: a Bayesian approach to the selection of pathways and genes. *Ann Appl Stat* 5: 1978–2002, 2011.
66. **Sullivan JM, Prewitt RL, Ratts TE.** Sodium sensitivity in normotensive and borderline hypertensive humans. *Am J Med Sci* 295: 370–377, 1988.
67. **Suzuki S, Tanaka T, Poyurovsky MV, Nagano H, Mayam T, Ohkubo S, Lokshin M, Hosokawa H, Nakayama T, Suzuki Y, Sugano S, Sato E, Nagao T, Yokote K, Tatsuno I, Prives C.** Phosphate-activated glutaminase (GLS2), a p53-inducible regulator of glutamine metabolism and reactive oxygen species. *Proc Natl Acad Sci USA* 107: 7461–7466, 2010.
68. **Svetkey LP, McKeown SP, Wilson AF.** Heritability of salt sensitivity in black Americans. *Hypertension* 28: 854–858, 1996.
69. **Taylor NE, Glocka P, Liang M, Cowley AW Jr.** NADPH oxidase in the renal medulla causes oxidative stress and contributes to salt-sensitive hypertension in Dahl S rats. *Hypertension* 47: 692–698, 2006.
70. **Terashima M, Kobayashi M, Motomiya M, Inoue N, Yoshida T, Okano H, Iwasaki N, Minami A, Matsuoka I.** Analysis of the expression and function of BRINP family genes during neuronal differentiation in mouse embryonic stem cell-derived neural stem cells. *J Neurosci Res* 88: 1387–1393, 2010.
71. **Tian Z, Greene AS, Usa K, Matus IR, Bauwens J, Pietrusz JL, Cowley AW Jr, Liang M.** Renal regional proteomes in young Dahl salt-sensitive rats. *Hypertension* 51: 899–904, 2008.
72. **Tian Z, Liu Y, Usa K, Mladinov D, Fang Y, Ding X, Greene AS, Cowley AW Jr, Liang M.** Novel role of fumarate metabolism in Dahl salt-sensitive hypertension. *Hypertension* 54: 255–260, 2009.
73. **Vrijenhoek T, Buizer-Voskamp JE, van der Stelt I, Strengman E, Sabatti C, Geurts van Kelle A, Brunner HG, Ophoff RA, Velman JA.** Recurrent CNVs disrupt three candidate genes in schizophrenia patients. *Am J Hum Genet* 83: 504–510, 2008.
74. **Wang H, Li SZ.** Efficient Gaussian graphical model determination under *G*-Wishart prior distributions. *Electron J Stat* 6: 168–198, 2012.
75. **Wang K, Li M, Haronarson H.** ANNOVAR: functional annotation of genetic variants from next-generation sequencing data. *Nucleic Acids Res* 38: e164, 2010.
76. **Weinberger MH.** Salt sensitivity of blood pressure in humans. *Hypertension* 27: 481–490, 1996.
77. **Yang C, Stingo FC, Ahn KW, Liu P, Vannucci M, Laud PW, Skelton M, O'Connor P, Kurth T, Ryan RP, Moreno C, Tsaih SW, Patone G, Hummel O, Jacob HJ, Liang M, Cowley AW Jr.** Increased proliferative cells in the medullary thick ascending limb of the loop of Henle in the Dahl salt-sensitive rat. *Hypertension* 61: 208–215, 2013.
78. **Zheleznova NN, Yang C, Ryan RP, Halligan BD, Liang M, Greene AS, Cowley AW Jr.** Mitochondrial proteomic analysis reveals deficiencies in oxygen utilization in medullary thick ascending limb of Henle in the Dahl salt-sensitive rat. *Physiol Genomics* 44: 829–842, 2012.
79. **Zheng C, Heintz N, Hatten ME.** CNS gene encoding astrotactin, which supports neuronal migration along glial fibers. *Science* 272: 417–419, 1996.

